



Gjøvik University College

HiGIA

Gjøvik University College Institutional Archive

Hartung, D., Pflug, A. & Busch, C. (2012) Vein Pattern Recognition Using Chain Codes, Spatial Information and Skeleton Fusing. In: Lecture Notes in Informatics, Sicherheit 2012: Sicherheit, Schutz und Zuverlässigkeit Beiträge der 6. Jahrestagung des Fachbereichs Sicherheit der Gesellschaft für Informatik e.V. (GI); 7.-9. März 2012, Darmstadt: Gesellschaft für Informatik, p. 245-156.

Please notice:

This is the publisher's pdf version.

***© Reprinted with permission from
Gesellschaft für Informatik***

Vein Pattern Recognition Using Chain Codes, Spatial Information and Skeleton Fusing

Daniel Hartung

Norwegian Information Security Laboratory (NISlab)
Høgskolen i Gjøvik, Teknologivn. 22, 2815 Gjøvik, Norway
daniel.hartung@hig.no

Anika Pflug

University of Applied Sciences Darmstadt - CASED, Haardtring 100,
64295 Darmstadt, Germany
anika.pflug@cased.de

Christoph Busch

Norwegian Information Security Laboratory (NISlab)
Høgskolen i Gjøvik, Teknologivn. 22, 2815 Gjøvik, Norway
christoph.busch@hig.no

Abstract: Vein patterns are a unique attribute of each individual and can therefore be used as a biometric characteristic. Exploiting the specific near infrared light absorption properties of blood, the vein capture procedure is convenient and allows contact-less sensors. We propose a new chain code based feature encoding method, using spacial and orientation properties of vein patterns. The proposed comparison method has been evaluated in a series of different experiments in single and multi-reference scenarios on different vein image databases. The experiments show a competitive or higher biometric performance compared to a selection of minutiae-based comparison methods and other point-to-point comparison algorithms.

1 Introduction

Intended to be a robust approach for liveness detection in fingerprint and hand geometry systems, vein recognition evolved to an independent biometric modality over the last decade. Classically the capturing process can be categorized as a near or a far infrared approach. Vein recognition systems based on the near infrared approach are exploiting differences in the light absorption properties of the de-oxygenated blood flowing in subcutaneous blood vessels and the surrounding tissue. Veins become visible, as seen in figure 1, as dark tubular structures. They absorb higher quantities of the near infrared light, that is commonly emitted by LEDs of the sensor, than the tissue. Alternatively in the far infrared approach the heat radiation of the body can be measured: the temperature gradient between the blood vessels carrying the warm blood and the tissue can be measured in this spectrum.

Vein scanners work contact-less, hence they are considered to be more hygienic than sys-

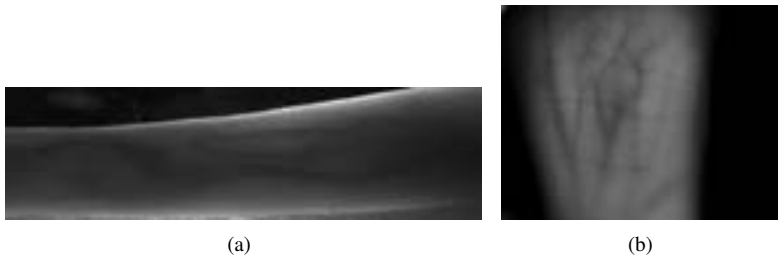


Figure 1: Finger / wrist vein samples images from: (a) GUC45; (b) UC3M database.

tems requiring direct physical contact.

Vein patterns evolve during the embryonic vasculogenesis, hence their final structure is mostly influenced by random factors [EYM⁺05]. Even though scientific research about the uniqueness of vein patterns is sparse, many sources state that vein patterns are unique among individuals. Because the network of blood vessels is located underneath the skin, a person's individual vein pattern is hard to forge. Furthermore, it is expected, that the position of veins is constant over a whole lifetime [DRC06]. Offering the same user convenience as fingerprints while being highly secure against forging, vein recognition has been applied in various fields of authentication and access control during the last years such as ATMs or airports.

Still vein recognition faces challenges: limitations in capturing *in vivo* images from the inside of the body, as well as ambient sunlight, temperature and varying skin properties like the pigmentation, or the thickness influence the image quality. As a result of all these factors the raw images can have a low contrast, contain strong noise and a non-uniform brightness. Sophisticated algorithms for the preprocessing like contrast enhancement and segmentation as well as the final feature extraction and comparison are necessary to handle the variations and the noise. In this paper we contribute a new chain code based feature extraction method and investigate its performance in combination with fusion techniques of image skeletons. The fusion aims at enhancing the biometric performance and the robustness against noise induced by errors during the preprocessing phase. Our approach is compared with minutiae-based feature extraction and a state-of-the-art holistic direct comparison approach.

After giving an overview over previously done work in section 2, we introduce two techniques for skeleton fusion at feature level. We introduce our chain code based feature extraction method in section 4 and present our experimental setup as well as the results in sections 5 and 6. Finally conclusions and future work can be found in section 7.

2 Related Work

Since the first suggestion of using the blood vessel network as a biometric characteristic was made, a large number of different techniques for extracting and comparing vein

patterns have been proposed. In [KK09] and [WZY06] Principal Component Analysis (PCA) is used for classification of vein patterns. Another statistical approach is presented by Xueyan *et al.* [XS08], who use moment invariants as descriptors for the layout of blood vessels in vein images.

Hartung *et al.* [HOXB11] apply spectral minutiae to vein pattern recognition. In the approach, which has originally been developed for feature representation in fingerprint images [XV08], the coordinates of minutiae points are transformed into the frequency domain and mapped in a polar-logarithmic grid. This representation is translations and scale invariant; rotations become translations. For comparison the spectra are shifted and compared at a correlation basis (SMLFR). Instead of comparing the minutiae locations Wang *et al.* computes the distances between all minutiae for feature extraction [WZY06].

In [WLC07] the bifurcation points of vein patterns are interpreted as endpoints of line segments. The line segments are then compared separately to each other and the similarity of two vein patterns is expressed by the line segment Hausdorff distance. In a later approach Wang *et al.* propose to apply the modified Hausdorff distance (MHD) to vein minutiae in [WLC08], where a perfect discrimination of the far infrared data could be achieved.

In the approach proposed by Chen *et al.* two comparison algorithms are proposed [CLW09]. The goal is to make direct comparison algorithms more robust against rotation. Therefore first an algorithm called Similarity-based mix-matching is proposed (SMM), which compares segmented images and image skeletons with each other. Because the segmented version of an image is more tolerant to outliers, the approach tolerates small rotations. They also propose a modified version of ICP where the registration error is used as a similarity measure.

In 2003 Miura *et al.* have proposed a method called repeated line tracking, which tracks the course of veins by tracking dark structures in the images from randomly chosen starting points [MNM04]. Yang *et al.* present a modified version of repeated line tracking which uses the information gathered during line following for deriving a probability map for vein location [YXL09]. Miura *et al.* [MNM07] outline another algorithm for vein pattern extraction, which exploits local differences in brightness. The algorithm is based on the assumptions, that veins are thick, dark tubular structures and detect local minimums of grey values.

3 Skeleton Fusing

In our approach skeletal images are the basis for feature extraction. Because of noise and poor contrast, these skeletons will differ, even though they are generated from the same biometric source. In order to improve their reliability and hence the reliability of the extracted features, we propose two different approaches for fusing multiple skeletons into a single one.

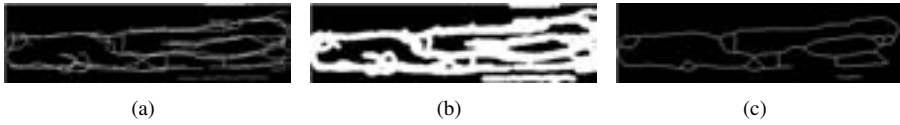


Figure 2: Fusion based on unification (GUC45 samples) using $n = 3$ input skeletons: (a) superimposed structure $S^{\text{uni}1}$; (b) disk-shape structuring element dilated structure $S^{\text{uni}2}$; (c) final unified skeleton S^{uni} .

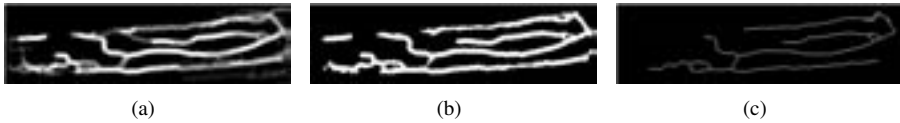


Figure 3: Fusion based on intersection (GUC45 samples) with $n = 5$ input skeletons and threshold $t = 3$: (a) dilated density structure $S^{\text{int}2}$; (b) $S^{\text{int}3}$ (threshold t applied to segment $S^{\text{int}2}$); (c) final intersection skeleton S^{int} .

3.1 Unified Skeleton

The first approach takes n input skeletons from the same biometric source and computes a unified skeleton based on the input. In a first step, all input skeletons $S_i(x, y)$ are aligned with each other using the Iterative Closest Points algorithm (ICP) [RL01] and then superimposed to a common structure S^{uni} (Fig. 2(a)):

$$S^{\text{uni}1}(x, y) = \cup_{i=1}^n S_i(x, y) \quad (1)$$

The registered input skeletons are fused by dilating the superimposed binary image $S^{\text{uni}1}$ with a disk-shaped structuring element (Fig. 2(b)) to get $S^{\text{uni}2}$. Afterwards the fast marching skeletonization algorithm [TvW02] is applied to the dilated image in order to create the unified skeleton S^{uni} (Fig. 2(c)).

3.2 Intersected Skeleton

The second proposed algorithm creates an intersected skeleton, which possesses only those features which occur in at least t of the n input skeletons. An example for skeleton intersection with $n = 5$ input skeletons is illustrated in Figure 3. The intersected skeleton in Figure 3 consists of the lines which occur in at least three of the five input skeletons ($t = 3$).

Similarly to the unification approach, the input skeletons S_i need to be aligned to each other. Afterwards each of the n input skeletons is dilated with a disk-shaped structuring element, creating binary structures $S^{\text{int}1}$. These dilated skeletons are then added up to form a common unified density structure called $S^{\text{int}2}$.

$$S^{\text{int}_2}(x, y) = \sum_{i=1}^n S_i^{\text{int}_1}(x, y) \quad (2)$$

S^{int_2} contains values between 0 and n at each location (x, y) . The interpretation: $S^{\text{int}_2}(x, y)$ represents the number of skeletons that are classified as veins in location (x, y) for the input skeletons – all input skeletons have a pixel that is classified as vein in case of $S^{\text{int}_2} = n$ and none if it is equal to 0.

Now a threshold value t with $1 \leq t \leq n$ is applied to S^{int_2} resulting in S^{int_3} . In this step all pixels which at least occur t times in the input skeletons are kept, all other pixels are set to zero.

$$S^{\text{int}_3}(x, y) = \begin{cases} 1 & \text{if } S^{\text{int}_2} \geq t \\ 0 & \text{else} \end{cases} \quad (3)$$

Finally the fast marching skeletonization is applied [TvW02], which results in the intersected skeleton S^{int} .

4 Chain Code Comparison

Similarities between two image skeletons can be determined by measuring the relative positions of the skeleton lines as well as their relative orientation. Two lines, which are parallel should be considered to be more similar than two non-parallel skeleton lines. The proposed feature extraction uses the position of each pixel on a skeleton line in combination with its local orientation reflected by the chain code value. Thus the algorithm finds associated points between the probe and the reference skeleton and measures its parallelism.

4.1 Preliminaries and Assignment

However before chain code values can be assigned to an image skeleton, some preliminaries have to be met. In a first step the probe and the reference skeleton have to be aligned with each other. As for skeleton fusion, we used ICP for skeleton alignment. Moreover all points where veins split up (bifurcations) have to be removed from the image skeleton in order to avoid ambiguities. These points are extracted with a fast convolution method [OHBL11] resulting in separated line elements.

To make sure all chain codes refer to a common starting point, a reading direction has to be defined. In our work, the chain code feature extraction module iterates over each pixel (x, y) of the skeleton starting from the bottom left corner of each line element and ends at the top right corner. Chain codes extracted from the same shape with different coordinates will be identical. Each skeleton pixel is assigned a chain code value according to the relative position of its successor, which is equivalent to the next skeleton pixel hit

when moving along the reading direction (see Figure 4). All skeletons are defined as 8-connected structures.

4.2 Comparison

After the chain code assignment for the reference and the probe, the similarity between two aligned chain codes C and C' can be calculated. The algorithm tries to find pairs of associated points in the reference and the probe. All skeleton points of the reference are used for the comparison in the following way: a search direction is defined for a skeleton pixel at (x, y) of the reference. It is orthogonal to the direction of the local orientation which is approximated by the chain code value stored at the examined point.

Starting from the same position (x, y) in the probe, the search for associated pixels stops if either an associated point could be found in the search direction or if the maximum search depth d_{max} is exceeded. When a pair of associated skeleton points has been found, their similarity is calculated based on their euclidean distance d and the chain code difference c , where (x, y) and (x', y') are the coordinates of the two associated points and $C(x, y)$ and $C'(x', y')$ are their chain code values.

$$d = \sqrt{|x - x'|^2 + |y - y'|^2}, \text{ and} \quad (4)$$

$$c = |C(x, y) - C'(x', y')|^2 \quad (5)$$

The local error E at point (x, y) is then calculated as follows:

$$E(x, y) = \frac{d + c}{E_{max}}, \text{ with} \quad (6)$$

$$E_{max} = d_{max} + c_{max} \quad (7)$$

The values for d_{max} and c_{max} denote the maximum search depth and the maximum possible difference between two chain code values. Following Equation 5 and the scheme sketched in Figure 4, $c_{max} = 8^2 = 64$. The local error is stored at position (x, y) in an error map E , which has the same size as the input images.

The assignment of associated points is not commutative and therefore the order of the two input skeletons leads to different results (probe/reference). Starting with the reference skeleton and searching for an associated pixel in the probe skeleton, a different pixel pair can be identified as the other way around. This is handled by computing two error maps E_1 and E_2 . E_1 contains all local errors calculated by using C as reference and C' as probe skeleton and E_2 contains all local error using C' as probe and C as reference, respectively. The total error map E_{total} is the sum of local errors for each point in the skeleton images and is computed as follows:

$$E_{total}(x, y) = E_1(x, y) + E_2(x, y) \quad (8)$$

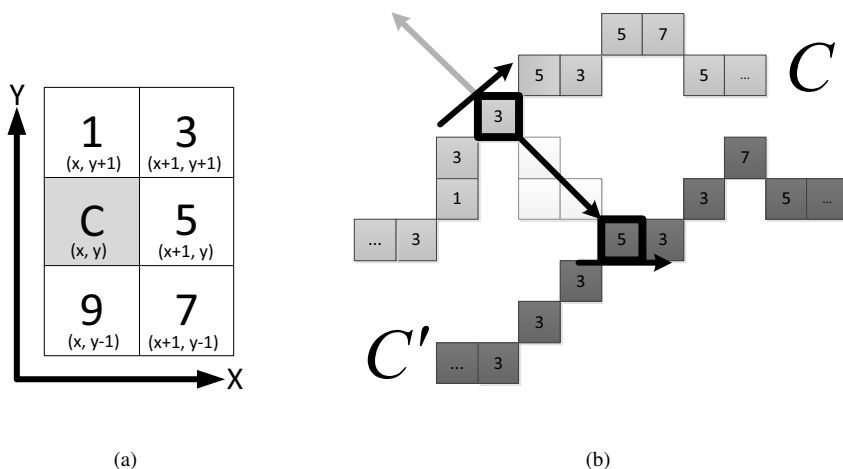


Figure 4: Chain code extraction scheme and search procedure for finding associated pixels.

Similarly the error map for the maximum possible error E_{lim} between the current image pair E_1 and E_2 is the sum of the maximum error values at each pixel in the skeleton images.

$$E_{lim}(x, y) = E_{1_{max}}(x, y) + E_{2_{max}}(x, y) \quad (9)$$

Finally the normalized similarity score of the comparison is defined as:

$$Score = 1 - \frac{\sum_x \sum_y E_{total}(x, y)}{\sum_x \sum_y E_{lim}(x, y)} \quad (10)$$

An example of how a point pair can be found by using the local chain code value is shown in Figure 4(b). The algorithm starts at the boldly bordered point in C and searches in orthogonal direction for a corresponding point in C' . After two mated points have been identified, their local error, which is a value between 0 (no error) and 2 (maximum error) is calculated. The global distance measure between all points in C and C' is, as stated before, the weighted sum of all local errors.

5 Experimental setup

The influence of using different feature extraction and comparison strategies including the proposed chain code based algorithm was measured using the Equal Error Rate (EER). Further, the influence of the proposed skeleton fusion techniques is quantified during the simulations.

5.1 Datasets

In the experiments two different vein databases were used. In both cases the images were captured with a CCD-camera and illuminated with NIR light at a wavelength of 850nm. The GUC45 dataset contains finger vein images from 45 data subjects collected at Gjøvik University College in Norway over a long period of time. Each finger, including the thumbs, was captured two times during each of the 12 sessions, which results in 10800 unique vein images in total. The image from GUC45 suffer from low contrast and high noise, which makes it hard for any algorithm to extract stable skeletons and hence to achieve a low error rate on this data. However this fact makes the images particularly interesting for research purposes as it allows for exploring the limitations of any algorithm for feature extraction and comparison.

The second database, called UC3M, consists of wrist vein images, which were collected as described in [PJUA⁺10]. The focus of this experiment was to evaluate the effect of different illumination intensities on the visibility of veins. For each of the 29 users, 6 images were taken for each hand under three different illumination settings. This results into 348 images in total.

5.2 Preprocessing

The preprocessing stage consists of three steps, namely image enhancement, segmentation and skeletonization. During image enhancement, noise should be removed and at the same time image contrast should be enhanced. In order to meet both criteria, different methods are combined. In a first step, the vein images are enhanced with adaptive non-local means as proposed by Struc and Pavesic [SP08] followed by non-linear diffusion for noise suppressing and edge enhancement [wei01].

The image enhancement step is followed by a segmentation step. In order to evaluate, if there is an image segmentation method, which is particularly suitable for segmenting vein images, three different segmentation methods have been benchmarked. The first of these methods is Otsu's histogram-based segmentation [Ots79]. Additionally the active contours algorithm proposed by Chan and Vese [CV01] and the multi-scale filter method by Frangi *et al.* [FNVV98] have been tested on the vein images.

Preprocessing is concluded by the skeletonization approach proposed by Telea and van Wijk [TvW02]. The advantage of this method is the built-in skeleton pruning, which allows cutting off small, noisy branches of the image skeleton.

5.3 Feature Extraction & Setup

All experiments were conducted on the basis of a modular vein verification system implemented in MATLAB. The benchmark system allows for arbitrary combinations of different

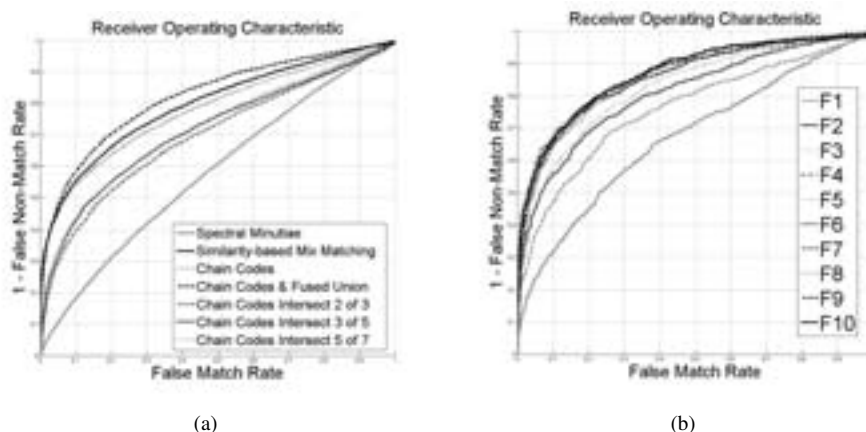


Figure 5: (ROC curves for (a) selection of feature extraction algorithms and (b) *Fused Union* configuration, different finger samples from GUC45 dataset. Finger indices are assigned according to the ISO-standard [ISO05] with indices 1 until 5 for the right hand fingers in indices 6 until 10 for the left hand fingers, where counting always starts from the thumbs.

preprocessing, feature extraction and comparison modules. We evaluated the performance of spectral minutiae (SMLFR) as proposed in [HOXB11], Similarity-based Mix-Matching (SMM) [CLW09] and the performance of chain code comparison on single references and fused skeletons. In all experiments using fusion techniques, the fused skeleton served as the reference image and a skeleton extracted from one vein image was used as the probe image.

6 Results

In our experiments, the segmentation algorithms came to slightly different performance results, but had a minor effect on the overall system's performance. The measured performance difference between the different segmentation algorithms is less than 2% points in terms of the EER. The main difference between the evaluated segmentation approaches was in terms of computation time, however the approach by Frangi and Niessen performed slightly better on the UC3M dataset.

In contrast to the preprocessing step, the impact of the feature extraction and comparison method is significant. We evaluated the performance of spectral minutiae (SMLFR) as proposed in [HOXB11], Similarity-based Mix-Matching (SMM) [CLW09] and the performance of chain code comparison on single references and fused skeletons. Table 1 summarized the performance measures for each of the datasets. The results for GUC45 were obtained using Otsu's segmentation algorithm, whereas the EER measures on UC3M are based on Frangi and Niessen's filter-based approach.

As stated before, the images in GUC45 have a particularly low contrast and therefore can-

Comparison Algorithm	GUC45	UC3M
Chain Codes	28.72	1.38
Fused Union	24.67	0.63
Fused Intersect $t=2, n=3$	34.19	0.69
Fused Intersect $t=3, n=5$	32.85	NA
Fused Intersect $t=5, n=7$	34.30	NA
SMM	27.84	1.38
SMLFR	40.25	5.90

Table 1: Benchmark results (EER in %) for finger vein (GUC45) and wrist images (U3CM). NA: not possible due to limited number of samples per source.

not be expected to give good biometric performance. However, GUC45 is a challenge for all tested algorithms. In addition, it also contains multiple samples per subject. The results of the different feature extraction and comparison approaches on GUC45 are summarized in Figure 5. The best performance could be achieved with chain code comparison using unified skeletons as reference samples and skeletons derived from only one image as probes. This configuration was named *Fused Union* and with an EER of 24.67% it outperformed all other configurations including SMM, but also single reference chain code comparison. This shows that already a simple skeleton fusing approach like the proposed one, enhances the quality of image skeletons and improves the system performance significantly.

Further investigations on the performance of Fused Union for each finger on GUC45 showed, that the fingers of the left hand performed better than the right hand fingers (see Figure 5(b)). In our experiments, the highest error rate was measured with images from the thumbs (Fingers indices 1 and 6). The EER of configurations using intersected skeletons gets higher the more input skeletons are used. A reason for this could be that unstable skeletons have only few intersecting parts, which results in fused skeletons with low complexity. Less details however mean less distinctive power and results in increasing error rates.

For the UC3M dataset an excellent biometric performance could be measured without the skeleton fusion techniques proposed. SMM and the chain code algorithm perform at the same level (around 1% EER). Skeleton fusion could reduce the EER to 0.63%, whereas skeleton intersection with $n = 3$ and $t = 2$ yielded in a slightly higher EER of 0.69%.

7 Conclusion and Future Work

The proposed chain code algorithm as well as the state of the art SMM algorithm perform very similar on the chosen datasets, it seems the quality of the images is a limiting factor here. Only a multi-reference approach could further improve the results.

Even though the proposed comparison on Fused Union skeletons showed promising re-

sults, the algorithm's time wise performance is not impressive compared to other feature extraction and comparison algorithms. Future work focuses on reducing the required computing time by replacing the pixel-based chain code extraction with a convolution-based approach and by selecting less reference points for skeleton registration and comparison. Further improvements could also be made by using a different error functions to make it less sensitive to single outliers and more sensitive to mismatching line segments. Moreover, additional simulations on different vein datasets will also show the feasibility of the approach for different vein modalities.

In summary the combination of spacial information and chain codes proved to be an interesting new technique, which combines the robustness and simplicity of holistic comparison methods with information about the local orientation of vein patterns. On the selection of vein data, chain code comparison performed competitive to state of the art holistic methods like SMM and superior to minutiae-based comparison (SMLFR). It can be easily extended to a multi-reference scenario: on the proposed Fused Union skeletons the performance is superior to the other algorithms.

References

- [CLW09] Haifen Chen, Guanming Lu, and Rui Wang. A New Palm Vein Method Based on ICP Algorithm. In *International Conference on Informaion Systems*, November 2009.
- [CV01] Tony F. Chan and Luminiatia Vese. Active Contours Without Edges. *IEEE Transactions on Image processing*, 10(2):266–277, February 2001.
- [DRC06] Reza Derakhshani, Arun Ross, and Simona Crihalmeanu. A New Biometric Modality Using Concunctival Vasculature. In *Proceedings of Artificial Neural Networks in Engineering*, November 2006.
- [EYM⁺05] Anne Eichmann, Li Yuan, Delphine Moyon, Ferdinand Lenoble, Luc Pardanaud, and Chinstiane Bréant. Vascular Development: From Precursor Cells to Branched Arterial and Venous Networks. *International Journal of Developmental Biology*, 49:259–267, 2005.
- [FNVV98] Ro F. Frangi, Wiro J. Niessen, Koen L. Vincken, and Max A. Viergever. Multiscale Vessel Enhancement Filtering. In *Medical Image Computing and Computer-Assisted Intervention*, pages 130–137. Springer-Verlag, 1998.
- [HOXB11] Daniel Hartung, Martin Aastrup Olsen, Haiyun Xu, and Christoph Busch. Spectral Minutiae for Vein Pattern Recognition. In *The IEEE International Joint Conference on Biometrics (IJCB)*, 2011.
- [ISO05] ISO/IEC 19795-1:2006 Information Technology *Biometric Data Interchange Formats - Part 2: Finger Minutiae Data*, March 2005.
- [KK09] Maleika Heenaye-Mamode Khan and Naushad Mamode Khan. Feature Extraction of Dorsal hand- Vein Pattern Using a Fast Modified PCA Algorithm Based on Cholesky Decomposition and Lanczos Technique. *International Journal of Mathematical and Computer Sciences*, 5(4):230–234, 2009.

- [MNM04] Naoto Miura, Akio Nagasaka, and Takafumi Miyatake. Feature Extraction of Finger-vein Patterns Based on Repeated Line Tracking and its Application to Personal Identification. *Machine Vision and Applications*, 15:194–203, Juli 2004.
- [MNM07] Naoto Miura, Akio Nagasaka, and Takafumi Miyatake. Extraction of Finger-Vein Patterns Using Maximum Curvature Points in Image Profiles. *IEICE - Transactions on Information and Systems*, E90-D(8):1185–1194, August 2007.
- [OHBL11] Martin Aastrup Olsen, Daniel Hartung, Christoph Busch, and Rasmus Larsen. Convolution Approach for Feature Detection in Topological Skeletons Obtained from Vascular Patterns. In *IEEE Symposium Series on Computational Intelligence 2011*, Apr 2011.
- [Ots79] Nobuyuki Otsu. A Threshold Selection Method from Grey-Level Histograms. *Systems, Man and Cybernetics, IEEE Transactions*, 9:62–66, January 1979.
- [PJUA⁺10] Suarez Pascual, J.E., Uriarte-Antonio, J., Sanchez-Reillo, R., and M.G. Lorenz. Capturing Hand or Wrist Vein Images for Biometric Authentication Using Low-Cost Devices. In *Intelligent Information Hiding and Multimedia Signal Processing (IIH-MSP), 2010 Sixth International Conference on*, pages 318–322, october 2010.
- [RL01] Szymon Rusinkiewicz and Marc Levoy. Efficient Variants of the ICP Algorithm. Technical report, Stanford University, 2001.
- [SP08] Vitomir Struc and Nikola Pavesic. Illumination Invariant Face Recognition by Non-local Smoothing. In *Proceedings of the BIOID Multicomm*, September 2008.
- [TvW02] Alexandru Telea and Jarke J. van Wijk. An Augmented Fast Marching Method for Computing Skeletons and Centerlines. In *Joint Eurographics - IEEE TCVG Symposium on visualization*, 2002.
- [wei01] *Applications of Nonlinear Diffusion in Image Processing and Computer Vision*, volume Vol. LXX. Acta Math. Univ. Comenianae, 2001.
- [WLC07] L. Wang, G. Leedhm, and S.-Y. Cho. Infrared imaging of Hand Vein Patterns for Biometric Purposes. *IET computer vision*, 1(3):113–122, 2007.
- [WLC08] Lingyu Wang, Graham Leedham, and David Siu-Yeung Cho. Minutiae feature analysis for infrared hand vein pattern biometrics. *Pattern Recognition*, 41(3):920 – 929, 2008. Part Special issue: Feature Generation and Machine Learning for Robust Multimodal Biometrics.
- [WZYZ06] Kejun Wang, Yan Zhang, Zhi Yuan, and Dayan Zhuang. Hand Vein Recognition Based on Multi Supplemental Features of Multi-Classifer Fusion Detection. In *International Conference on Mechatronics and Automation*, June 2006.
- [XS08] Li Xueyan and Guo Shuxu. *Pattern Recognition Techniques: Technology and Applications*, chapter The Fourth Biometric, page 626 ff. I-Tech, 2008.
- [XV08] Haiyun Xu and Raymond N.J. Veldhuis. Spectral Minutiae: A Fixed-length Representation of a Minutiae Set. In *IEEE Computer Society Conference on Computer Vision and Pattern Recognition Workshops*, pages 1–6, 2008.
- [YXL09] Wenming Yang, Xiang Xu, and Quingmin Liao. Personal Authentication Using Finger Vein Patterns and Finger-Dorsa Texture Fusion. In *MM '09 Proceedings of the 17th ACM international conference on Multimedia*, 2009.